[12]M. Hansen, *Constitution of Binary Alloys* (McGraw-Hill, New York, 1958).
[13]D. T. Keating, W. T. Neidhardt, and A. N. Goland, Phys. Rev. 111, 261 (1958).
[14]We are indebted to D. J. Sellmyer for these susceptibility measurements.
[15]M. D. Daybell and W. A. Steyert, Phys. Rev. Letters 18, 398 (1967); C. M. Hurd, Cryogenics 6, 264 (1966); J. Phys. Chem. Solids 28, 1345 (1967); Phys. Rev. Letters 18, 1127 (1967).
[16]J. L. Tholence and R. Tournier, Phys. Rev. Letters 25, 867 (1970).
[17]J. M. Franz, thesis (M.I.T., 1971) (unpublished); J. M. Franz and D. J. Sellmyer (private communication).
[18]A. J. Heeger, L. B. Wels, M. A. Jensen, and G. Gladsone, Phys. Rev. 172, 302 (1968).
[19]A. J. Appelbaum and J. Kondo, Phys. Rev. Letters 19, 906 (1967); Phys. Rev. 170, 542 (1968).
[20]D. C. Golibersuch and A. J. Heeger, Phys. Rev. 182, 584 (1969).
[21]N. Rivier and M. J. Zuckermann, Phys. Rev. Letters 21, 904 (1968).

PHYSICAL REVIEW B VOLUME 5, NUMBER 3 1 FEBRUARY 1972

Magnetism in Amorphous Fe-Pd-P Alloys*

T. E. Sharon and C. C. Tsuei
W. M. Keck Laboratory of Engineering Materials, California Institute of Technology, Pasadena, California 91109
(Received 30 August 1971)

Amorphous alloys of composition $Fe_xPd_{80-x}P_{20}$ ($13 \leq x \leq 44$) have been prepared by rapid quenching from the liquid state. The Mössbauer effect in Fe^{57} has been used to study the magnetic properties of these materials. The hyperfine field distribution has been determined from these experiments, as a function of composition and temperature. The results indicate that the electronic state of Fe in these alloys remains essentially constant throughout the composition range, and that the Pd *d* band is filled by electron transfer from phosphorus. The variation of the magnetic transition temperature with composition has been determined by combining the Mössbauer-effect results with complementary magnetic measurements. There is a sharp change in slope in this curve at $x \simeq 26$. Below this concentration, the long-range magnetic order which prevails in the higher-Fe-concentration alloys breaks down, giving rise to a more local ordering. The Mössbauer-effect results confirm the existence of weakly coupled Fe atoms in all the amorphous Fe-Pd-P alloys. These atoms reside in low effective fields, and can participate in the spin-flip–scattering process which produces a Kondo effect (resistivity minimum). The large critical concentration observed is also an indication that the spin correlations are greatly reduced in these amorphous alloys.

I. INTRODUCTION

One topic of current interest in the field of magnetism is the problem of the magnetization of an amorphous material. Although the concept of an amorphous ferromagnet was introduced by Gubanov[1] over a decade ago, only in the last few years has the subject become an area of active experimental research. The existence of amorphous ferromagnets has been confirmed by conventional magnetic measurements[2–5] and supporting Mössbauer-effect data.[6] Thus far the problem of magnetism in an amorphous alloy system (one in which the concentration of the magnetic element can be varied) has received less attention.[7,8] This is partly due to the fact that success in obtaining an amorphous structure has usually been limited to a rather narrow composition range.

In order to make a meaningful study of the composition dependence of the magnetic properties of an amorphous alloy system, it is essential that a continuity of structure extends throughout the composition range. Although an amorphous material has no long-range order (translational symmetry), it does possess definite structural properties based on its short-range order. These are reflected in the radial distribution function (RDF) which is obtained from x-ray diffraction analysis, and form the basis for any discussion of the properties of an amorphous alloy. This requirement of structure continuity parallels that in a crystalline alloy system, where one demands that all the alloys are of the same phase.

The structure of an amorphous Fe-Pd-P alloy system has recently been studied by Maitrepierre.[9,10] It was shown that alloys of composition $Fe_xPd_{80-x}P_{20}$, where $13 \lesssim x \lesssim 44$, can be quenched from the liquid state into an amorphous state using the "piston and anvil" technique.[11] It was found from the RDF data that the short-range order in these alloys is continuous with respect to variations in iron concentration, and that iron and palladium appear to substitute freely in this structure. Maitrepierre has suggested that the short-range

order in these alloys is based on the kind of structural units found in the metal-rich transition-metal phosphides (Pd_3P or Fe_3P).[12] In preliminary magnetization measurements, the saturation moment in a field of 8.4 kOe and at 4.2 °K decreased in roughly a linear fashion from 2.1 μ_B ($Fe_{33}Pd_{36}P_{20}$) to 0.6 μ_B ($Fe_{13}Pd_{67}P_{20}$). The higher-iron-concentration alloys were judged to be ferromagnetic by conventional criteria, but the low-iron-concentration alloys ($x \lesssim 25$) showed a more complex behavior. No Curie point could be defined from the magnetization data, and the effective moment in the paramagnetic region was quite large ($\mu_{eff} \sim 6\mu_B$). These observations led Maitrepierre to suggest the existence of "superparamagnetism" in these alloys.

Another somewhat puzzling effect observed in the electrical properties of the amorphous Fe-Pd-P alloys is the existence of a Kondo-type resistivity minimum[13] in even the most iron-rich compositions. This is surprising because normally, in a crystalline system, only a few atomic percent of the magnetic impurity causes correlations between the spins which suppress the spin-flip scattering responsible for the Kondo effect. If the phenomenom of the resistivity minimum is really due to this process, this suggests that the correlations between neighboring spins in an amorphous material are significantly reduced compared to the crystalline state.

In the present work, a more detailed study of the magnetism in this amorphous alloy system has been carried out, utilizing the Mössbauer-effect and other magnetic measurements. There are several reasons for applying Mössbauer spectroscopy to the study of the magnetic properties of these amorphous alloys. This method permits examination of the properties of single atoms, rather than complicated assemblages of atoms as in magnetization measurements. The latter results are difficult to interpret if a complicated and perhaps unknown spin arrangement exists. Bulk magnetic measurements cannot answer either the question of whether all the moments are aligned to the same extent, or whether there is a continuous distribution in the degree of alignment. The Mössbauer effect has proven to be a unique tool for the measurement of such magnetic field distributions.[14] In amorphous alloys this asset should be quite valuable.

A second important reason for applying the Mössbauer technique is that no external field need be applied to the sample. The bulk magnetic properties of a material are greatly influenced by such factors as domain structure, grain size, heat treatment, and many other such effects. At present these factors are poorly understood for amorphous materials. In the Fe-Pd-P alloys, for example, even in the highest field (8.4 kOe) and lowest temperatures (4.2 °K) used, the alloys appeared magnetically unsaturated.[9] This means that the conventional techniques[15] used to find the zero-field magnetization, which is the quantity of real interest, are either inapplicable or of questionable accuracy. Furthermore, the application of large external fields is undesirable because the microscopic spin ordering may change in response to this perturbing influence.

II. EXPERIMENTAL PROCEDURES

The amorphous Fe-Pd-P alloys were obtained by rapid quenching from the liquid state using the "piston and anvil" technique.[11] Initially, appropriate quantities of iron (99.9% purity), palladium (99.99% purity), and reagent-grade red amorphous phosphorus powder were combined into briquets by a sintering process. These were then induction melted in an argon atmosphere and drawn into 2-mm rods. The rods were then broken into pieces of appropriate size for use in the quenching process. Full details of the alloy preparation may be found elsewhere.[9,10]

Because actual cooling rates may vary from sample to sample, each sample was carefully checked by a step-scanning diffractometer to ensure that only the broad bands indicative of an amorphous structure were present. If a sample showed any weak Bragg reflections superimposed on this background, it contained some crystalline phase and was rejected for use in further experimental work.

The resulting quenched samples are foils approximately 2 cm in diameter and 40–50 μ thick. For use as Mössbauer absorbers, the foils are somewhat thick. This results in high absorption and a relatively small resonant effect. It was thought unwise to thin the foils by mechanical or chemical treatment, however, because of the unknown effect on their properties. In several cases the brittleness of the foils made such a procedure unfeasible anyway.

Two Fe-Pd-P alloys used by Maitrepierre were subjected to a chemical analysis after sintering.[9] It was found that the actual compositions of all three elements were within 0.5 at.% of the nominal ones. The small weight loss after melting (< 0.2%) also indicates that it is reasonably accurate to designate the samples by their nominal compositions, hence we do so in any further discussion.

A standard Mössbauer spectrometer[16] operating in the constant-acceleration mode was used to collect the data. The source was Co^{57} in Cu, which gave a linewidth of 0.28 mm/sec when used with a thin Fe absorber. Experiments at room temperature, where a simple two-peak spectrum is observed for all but one of the compositions, required data collection for about 8 h. In the low-temperature apparatus, both source and absorber

are cooled. In this case, the increased source to detector distance and absorption from coolants and Dewar windows required that data be collected for a longer period. Hence for all but the liquid-He experiments data were collected for several days. The statistics for the liquid-He experiments are noticeably poorer due to the reduced collection time.

In order to study the samples at several different temperatures, liquid helium and nitrogen, as well as dry-ice–acetone slushes and ice-water solutions, were used. These coolants provided temperatures of 4.2, 77, 194, and 273 °K, respectively. Room-temperature experiments correspond to 295 °K. Above room temperature a specially designed oven was used to provide continuous temperature control with a stability of about ± 0.5 °K.

After each set of experiments an Fe foil was used to provide the velocity calibration. The data were least-squares fitted to a six-peak spectrum and the line splittings of Preston *et al.*[17] were used to calculate the full-scale velocity.

Two additional techniques were used to detect magnetic transitions. Both rely on the change in the bulk magnetic properties of a sample as it becomes magnetically ordered. In one method (hereafter called frequency measurement) the sample was cut into the shape of a doughnut and many turns of fine wire wrapped around it to increase its inductance. This toroid was then used as the inductor in an LC oscillator, whose frequency of oscillation was measured as a function of temperature.

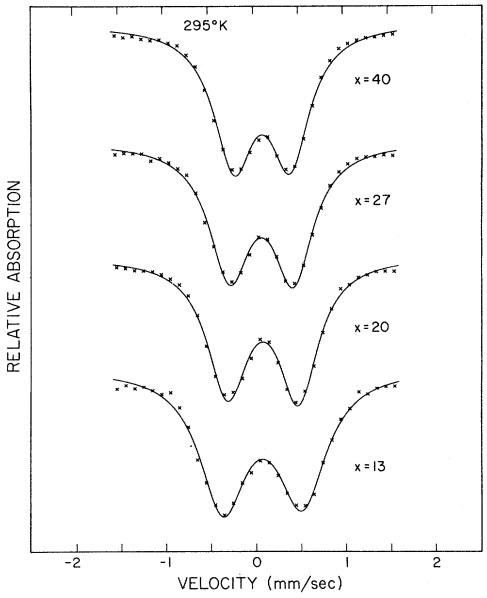

FIG. 1. Typical Mössbauer spectra for the amorphous $Fe_xPd_{80-x}P_{20}$ alloys at room temperature (295 °K).

The transition temperature was easily recorded for the higher-Fe-concentration ($x \gtrsim 25$) samples by taking readings from a frequency meter. For the lower-Fe-concentration samples, only a very small effect was observed at the transition temperature by this method. For these samples use was made of a very sensitive inductance bridge designed for detecting superconducting transition temperatures.[18] This system is capable of detecting transitions in only a few milligrams of superconducting material.

III. EXPERIMENTAL RESULTS AND DATA ANALYSIS

A. Mössbauer Effect

1. *Room-Temperature Results*

Typical Mössbauer spectra for the amorphous Fe-Pd-P alloys at room temperature (295 °K) are shown in Fig. 1. A sufficient condition for the absence of quadrupole splitting is cubic symmetry at each Fe site. Since the amorphous alloys obviously do not satisfy this criterion, the two-peak spectrum is expected. At this temperature only the highest-Fe-concentration alloy ($Fe_{44}Pd_{36}P_{20}$) studied shows evidence of magnetic splitting. The experimental data were fitted to two Lorentzian peaks of equal areas. The widths were allowed to vary to allow for some correlation between isomer shift and quadrupole splitting, which would produce an asymmetrical spectrum. The width difference for almost all the samples was found to be quite small (< 0.01 mm/sec), thus the spectra are nearly symmetric.

Figures 2–4 show the parameters obtained by a least-squares fitting using this approach. The large broadening observed is characteristic of the large scatter in isomer shifts and field gradients which exist in the amorphous material. The values obtained for the $Fe_{44}Pd_{36}P_{20}$ alloy are extrapolations from experiments just above the Curie point (321 °K).

In Fig. 4 no attempt is made to draw a smooth line through the data, since the linewidth depends on such factors as foil thickness and vibrational broadening which are not easily controlled.

2. *Low-Temperature Results*

The principal complication involved in applying the Mössbauer technique in the magnetically ordered amorphous alloys is that because of the variety of local environments possible, one can no longer speak of a unique hyperfine field or isomer shift for all the Fe nuclei in the solid. Instead, one must discuss these quantities on a statistical basis and give appropriate probability distributions. A secondary complication comes from the presence of a combined electric quadrupole and magnetic interaction and the lack of rotational symmetry,

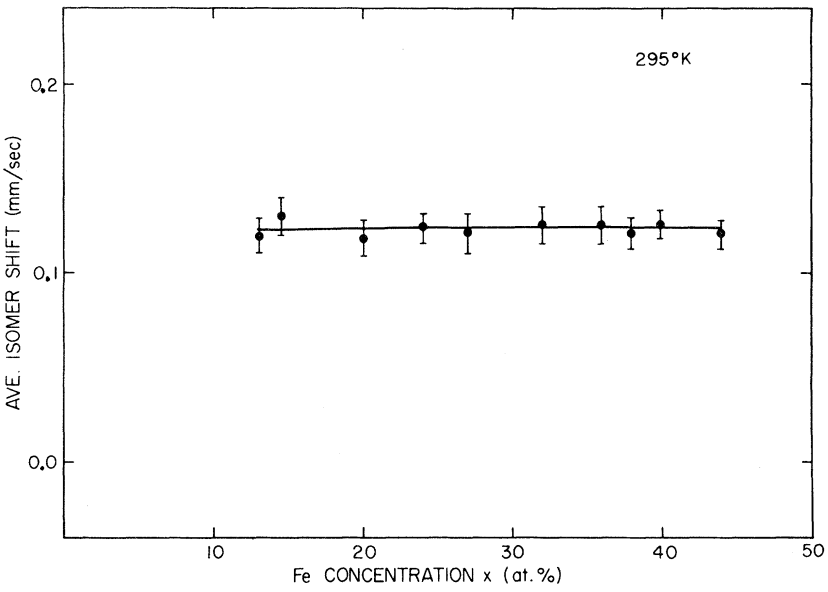

FIG. 2. Isomer shift vs iron concentration for the amorphous $Fe_xPd_{80-x}P_{20}$ alloys.

which would ordinarily imply quite lengthy numerical calculations even for a crystalline material. As we shall discuss now, in the present case the latter factor is not a major problem in interpreting the Mössbauer spectrum well below the transition temperature. In the magnetically ordered state which prevails at low temperatures, the magnetic moments of the iron atoms are aligned over a range considerably larger than interatomic distances. The electric field gradient (efg), on the other hand, is primarily determined by neighboring atoms within a few interatomic distances. The metallic nature of these alloys ($\rho \sim 3\rho_{Pd}$ at room temperature) prevents the existence of long-range electrostatic effects. The local principal axis of the efg cannot be obtained over any significant distance because of structural fluctuations. This means that on the average over the region of magnetic ordering, the efg principal axis and magnetic field are at random angles. In the higher-Fe-concentration samples which are ferromagnetic, this argument is closely related to the fact that the anisotropy constant K should be very small.

At any given Fe site there is, in general, no axial symmetry of the efg. Nevertheless, since there is no preferred direction on the average in an amorphous material, the most probable value of

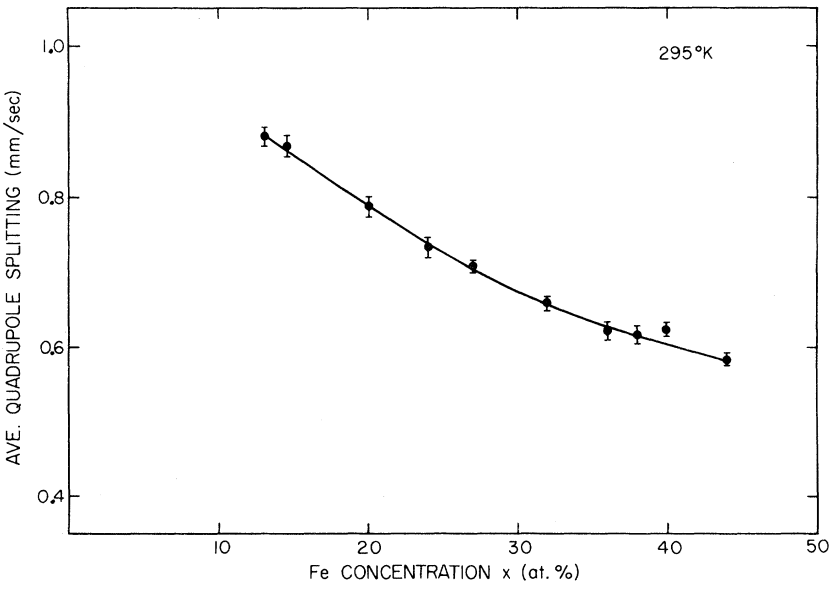

FIG. 3. Quadrupole splitting vs iron concentration for the amorphous $Fe_xPd_{80-x}P_{20}$ alloys.

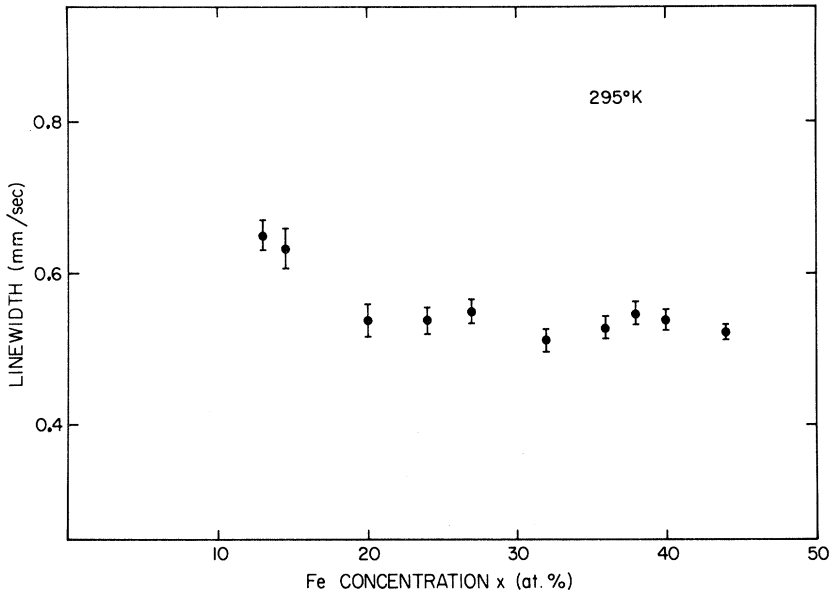

FIG. 4. Linewidth vs iron concentration for the amorphous $Fe_xPd_{80-x}P_{20}$ alloys.

$$\eta = (V_{xx} - V_{yy})/V_{zz}$$

is zero. A value of $\eta = 1$ (V_{xx} or $V_{yy} = 0$) would imply a very definite local order of atoms, and would be unlikely in an amorphous material. Assuming then, that $\eta \sim 0$, the excited-state energy levels are given by[19]

$$E(m) = -g\mu_N Hm + (-)^{|m|+1/2} \tfrac{1}{4} e^2 qQ \left[\tfrac{1}{2}(3\cos^2\theta - 1)\right] \quad (1)$$

provided $\mu H \gg e^2 qQ$. Since θ in the present case has a uniform distribution over the solid angle and $\langle \cos^2\theta \rangle_\Omega = \frac{1}{3}$, the average line positions due to the magnetic interaction will be maintained.

Only a slight broadening and distortion of line shape will result. The broadening from this effect and also a possible distribution of isomer shifts can be taken into account approximately by an increase in the linewidth. The Mössbauer spectrum can therefore be fitted in terms of a distribution of hyperfine fields $P(H)$, an average isomer shift δ, and a linewidth Γ.

To determine the form of the hyperfine field distribution we can consider a model in which the hyperfine field at a given Fe site is a function of the number of phosphorus nearest neighbors. Electron transfer from these atoms to the $3d$ shell of Fe should reduce the moment and hyperfine field. Assuming that this effect can be represented by an empirical rule

$$H = H'(1 - \alpha n) , \quad (2)$$

where n is the number of nearest-neighbor phosphorus atoms, we illustrate in Fig. 5 a possible hyperfine field distribution for close packing (12 nearest neighbors), with 20% of the sites randomly occupied by phosphorus. The constant H' is taken as 300 kOe (appropriate to Fe Pd alloys[20]) and $\alpha = 0.06$. The probabilities of a configuration with n nearest-neighbor phosphorus atoms is then given by the binomial distribution

$$P(n) = \binom{12}{n} (0.2)^n (0.8)^{12-n} . \quad (3)$$

These values and their corresponding hyperfine fields are represented by the vertical bars of Fig. 5. To allow for the amorphous nature of the material, we now allow α to assume a range of values, corresponding to the fluctuations in interatomic distances and next-nearest-neighbor effects. These are illustrated schematically in Fig. 5. We might then attempt to fit the experimental

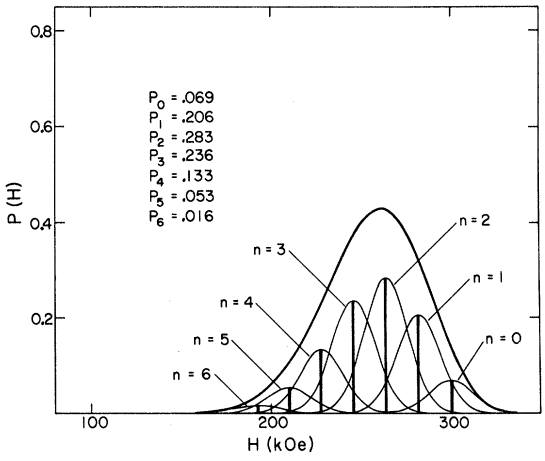

FIG. 5. Illustration of possible hyperfine field distribution in an amorphous material.

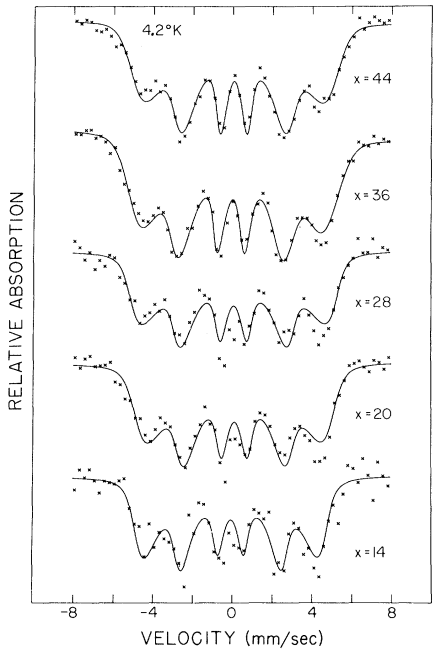

FIG. 6. Mössbauer spectra of the amorphous $Fe_xPd_{80-x}P_{20}$ alloys at 4.2 °K. The experimental points are shown and the fitting based on Eq. (4).

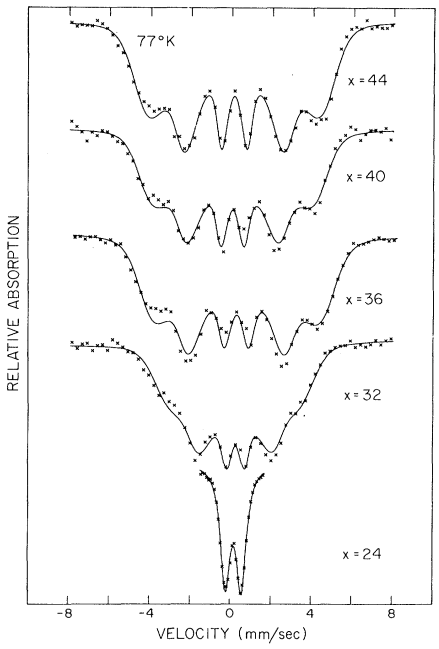

FIG. 8. Mössbauer spectra of the amorphous $Fe_xPd_{80-x}P_{20}$ alloys at 77 °K.

data on the basis of the most probable configurations. This was the approach followed by Tsuei *et al.*[6] in discussing an amorphous $Fe_{80}P_{12.5}C_{7.5}$ alloy. They used five average hyperfine fields with a Lorentzian distribution about each value and achieved a good fit of the experimental data.

For the amorphous Fe-Pd-P alloys, the approach was considered but not used for several reasons. First, the number of parameters is large and these parameters vary unpredictably. In particular, the

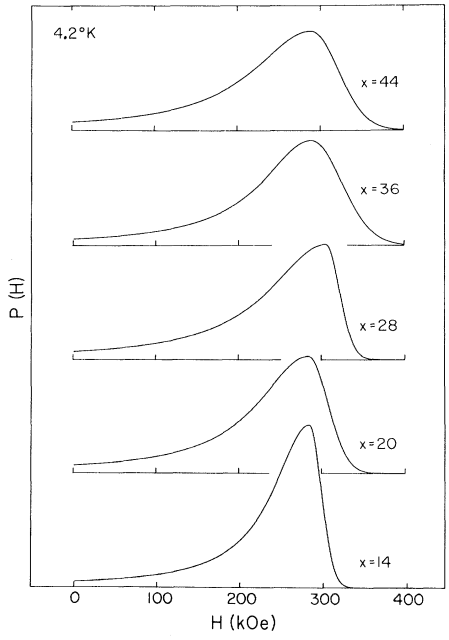

FIG. 7. Hyperfine field distributions corresponding to the fittings of Fig. 6. The vertical scale is the same for all the curves.

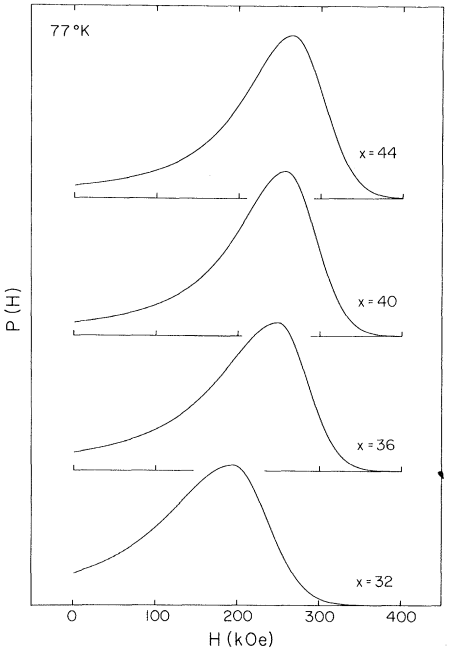

FIG. 9. Hyperfine field distributions corresponding to the fittings of Fig. 8.

TABLE I. Parameters obtained from analysis of Mössbauer-effect data at 4.2 °K based on Eq. (4). Estimated standard deviations are shown in parentheses. The symbols δ and Γ refer to the average isomer shift and linewidth, respectively.

Composition	δ (mm/sec)	Γ (mm/sec)	H_0 (kOe)	Δ_0 (kOe)	Δ_1 (kOe)
$Fe_{44}Pd_{36}P_{20}$	0.102(0.017)	0.447(0.047)	288.4(4.5)	171.8(11.0)	33.3(2.9)
$Fe_{36}Pd_{44}P_{20}$	0.108(0.016)	0.523(0.046)	287.7(3.8)	146.6(8.3)	36.8(2.9)
$Fe_{28}Pd_{52}P_{20}$	0.085(0.030)	0.553(0.095)	304.9(13.7)	167.0(17.1)	16.8(11.3)
$Fe_{24}Pd_{56}P_{20}$	0.076(0.020)	0.444(0.055)	296.6(4.8)	167.6(12.5)	20.0(3.4)
$Fe_{20}Pd_{60}P_{20}$	0.080(0.021)	0.570(0.069)	284.2(6.7)	148.5(11.1)	23.2(6.3)
$Fe_{14}Pd_{66}P_{20}$	−0.043(0.052)	0.554(0.181)	283.2(21.4)	106.0(26.2)	14.6(19.9)

intensities for the various configurations do not always agree well with a binomial distribution. The large number of parameters makes the numerical analysis quite lengthy and expensive in computer time. Second, the lack of detailed structure in the spectra of these alloys makes it unlikely that a unique fitting based on a certain number of configurations can be achieved.

It was decided, therefore, to base the analysis on a continuous distribution of hyperfine fields. In the simple model of Fig. 5 this is equivalent to replacing the seven individual curves by their sum, which is the solid top curve.

As a first attempt, a Gaussian distribution of fields was assumed to fit the experimental data. From the simple model of Fig. 5 this would appear to be a fair approximation. It was found using this approach, however, if the outer peaks were fitted well, the predicted absorption in the central part of the spectrum was much lower than was actually observed. This implies that there are significant contributions to the absorption coming from Fe sites with small hyperfine fields. The actual distribution therefore has a "tail" on the low-field side. In the numerical calculation, the following empirical formula was found to well represent the $P(H)$ functional form:

$$P(H) \propto \begin{cases} 1/[(H-H_0)^2 + \tfrac{1}{4}\Delta_0^2], & 0 \leq H \leq H_0 \\ e^{-(H-H_0)^2/2\Delta_1^2}, & H > H_0 . \end{cases} \quad (4)$$

The two forms are matched in value at $H = H_0$, and $P(H)$ is normalized numerically so that

$$\int_0^\infty P(H)\, dH = 1 .$$

Typical fittings achieved with this model are shown as solid lines in Figs. 6 and 7, and the corresponding field distributions in Figs. 8 and 9. In Tables I and II the parameters obtained by a least-squares analysis are given.

As the temperature increases and approaches the transition temperature, the Mössbauer spectrum narrows and the hyperfine field distribution shifts to lower fields (Figs. 10 and 11). It is clear that the procedure used thus far is not valid near T_c. First, the approximation $\mu H \gg e^2qQ$ is not satisfied and not valid in this region. Also the spectrum of a distribution of fields will approach a single peak instead of a quadrupole-type spectrum as T approaches T_c.

In Fig. 12 the Mössbauer spectrum of amorphous $Fe_{44}Pd_{36}P_{20}$ is shown in the vicinity of the transition temperature ($T_c \simeq 320$ °K). Two questions of importance to the magnetic properties of these alloys are how rapidly does the average hyperfine field approaches zero in this region and how well defined is the transition temperature actually. An exact analysis of the Mössbauer spectrum in this region is much too complicated.

The approach to be followed here is similar to that used by Dunlap and Dash[21] in their analysis of Co *Pd* alloys by a thermal scanning technique. In their experiments the full Mössbauer spectrum was not measured, but only the transmission rate with fixed source and absorber as a function of temperature near the Curie point. The problem here is complicated by the fact that a distribution of hyperfine fields exists even at $T = 0$ °K, and by the lack of cubic symmetry.

For simplicity in the analysis, the average value of the hyperfine field obtained at 4.2 °K (well below all Curie points) is assigned to each Fe atom as its saturation value. Around each Fe atom we consider a cell in which the magnetization is de-

TABLE II. Parameters obtained from analysis of Mössbauer-effect data at 77 °K based on Eq. (4).

Composition	δ (mm/sec)	(mm/sec)	H_0 (kOe)	Δ_0 (kOe)	Δ_1 (kOe)
$Fe_{44}Pd_{36}P_{20}$	0.098(0.009)	0.500(0.027)	265.9(2.4)	152.0(5.24)	38.5(1.8)
$Fe_{40}Pd_{40}P_{20}$	0.133(0.005)	0.643(0.017)	257.4(1.7)	151.8(2.5)	36.9(1.5)
$Fe_{36}Pd_{44}P_{20}$	0.070(0.011)	0.511(0.032)	248.0(3.3)	183.7(6.9)	36.5(2.7)
$Fe_{32}Pd_{48}P_{20}$	0.111(0.018)	0.495(0.046)	194.2(6.6)	210.4(4.6)	42.9(5.4)

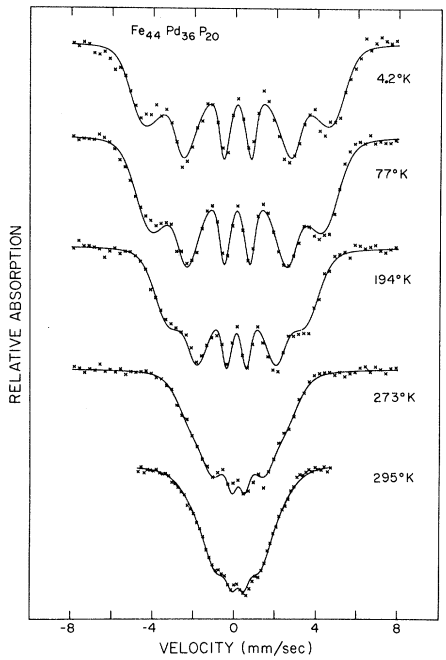

FIG. 10. Temperature dependence of the Mössbauer spectrum for the amorphous $Fe_{44}Pd_{36}P_{20}$ alloy. The solid curves are the fittings based on Eq. (4).

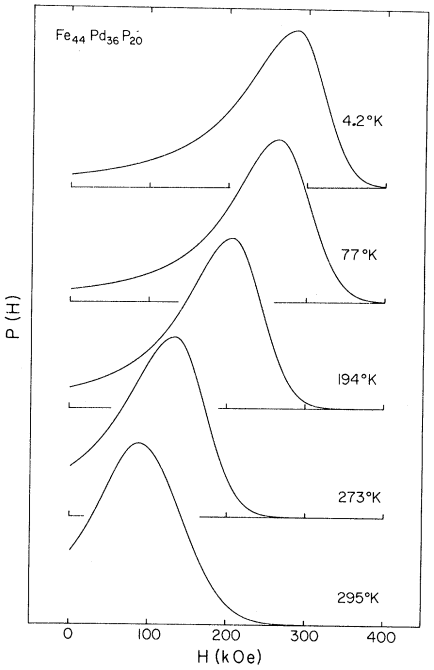

FIG. 11. Temperature dependence of the hyperfine field distribution for the amorphous $Fe_{44}Pd_{36}P_{20}$ alloy.

termined by the local concentration of Fe atoms and the temperature. The Fe atoms are assumed to be distributed throughout the material in a random fashion. If the cell has N atoms altogether then the probability of finding n Fe atoms is

$$P(n)=\binom{N}{n}x^n(1-x)^{N-n}\,. \tag{5}$$

For a reasonable size cell (more than 50 atoms) we can write to an excellent approximation

$$P(n)\cong 1/[2\pi\bar{n}(1-x)]^{1/2}e^{-(n-\bar{n})^2/2\bar{n}(1-x)}\,, \tag{6}$$

where $\bar{n}=xN$ is the average number of Fe atoms per cell.

The local Curie temperature is assumed to be a function of n. Since the experimental results indicate a fairly well-defined transition, the transition temperature of a cell does not vary too rapidly with n. Thus

$$T_c(n)\cong T_c(\bar{n})+\left(\frac{dT_c}{dn}\right)_{n=\bar{n}}(n-\bar{n})+\cdots\,. \tag{7}$$

Letting $T_c(\bar{n})=\bar{T}_c$ and $(dT_c/dn)_{n=\bar{n}}=a$, we obtain

$$P(T_c)=1/[2\pi\Delta T_c)^2]^{1/2}e^{-(T_c-\bar{T}_c)^2/2(\Delta T_c)^2}\,, \tag{8}$$

where $(\Delta T_c)^2=a^2\bar{n}(1-x)$. ΔT_c is a direct measure of the width of the transition.

To calculate the hyperfine field distribution we further assume that $H(T)/H(0)$ and $M(T)/M(0)$ vary with temperature for each cell according to the molecular field approximation[22]:

$$\frac{H(T)}{H(0)}=\frac{M(T)}{M(0)}=B_s\left(\frac{3S}{S+1}\,\frac{M(T)/M(0)}{T/T_c}\right)\,, \tag{9}$$

where

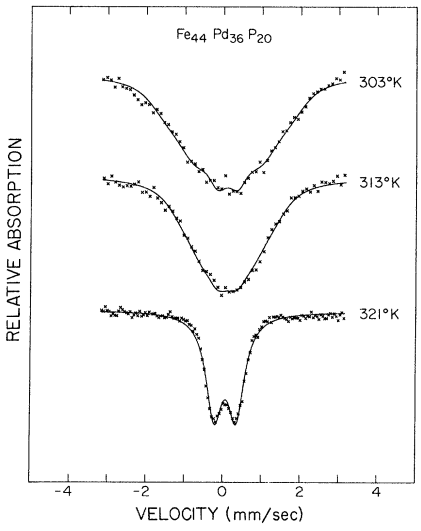

FIG. 12. Mössbauer spectra of the $Fe_{44}Pd_{36}P_{20}$ alloy near the transition temperature.

TABLE III. Parameters obtained from analysis of Mössbauer spectra near the transition temperature.

Composition	Temperature (°K)	$\bar{T}_c$(°K)	ΔT_c(°K)	$\bar{H}$(kOe)
$Fe_{44}Pd_{36}P_{20}$	303	317.7	7.98	63.4
$Fe_{44}Pd_{36}P_{20}$	313	319.3	3.71	46.0
$Fe_{44}Pd_{36}P_{20}$	316	319.7	2.25	33.6

$$B_s(x)=\frac{2S+1}{2S}\coth\left(\frac{2S+1}{2S}\,x\right)-\frac{1}{2S}\coth\frac{x}{2S}$$

is the Brillouin function for spin S. From the temperature of the experiment, the average Curie temperature T_c, and ΔT_c, it is possible to calculate the hyperfine field distribution and the resulting Mössbauer spectrum. To analyze the experimental data, $\bar{T}_c$ and ΔT_c are treated as parameters to be varied to best fit the data. Once they have been determined, the average hyperfine field can also be calculated. Table III gives the parameter values obtained from the experimental data of Fig. 12 using $S=1$. These results are typical of those seen in the lower-Fe-concentration samples, indicating a rather well-defined magnetic transition with a width of the order of a few degrees.

B. Variation of Transition Temperature with Fe Concentration

The Mössbauer results just described give several transition temperatures directly, and place upper and lower bounds on the rest. To give a more precise value to these intermediate points, the inductance measurements described earlier were used. For those alloys with $x \geq 28$ ($T_c > 77$ °K), the results obtained are in agreement with Mössbauer-effect results, in view of the experimental uncertainty in the exact composition of the foils. Results of the frequency measurements for foils in this range are typical of a ferromagnetic material, in which a large and sudden decrease in inductance at the Curie point is observed. This change occurs over a temperature interval of a few degrees, in approximate agreement with Mössbauer results, as shown in Fig. 13 for a $Fe_{28}Pd_{52}P_{20}$ amorphous alloy.

For the alloys of composition $x \leq 24$, a dramatic change in the nature of the effect is seen. The change in frequency or inductance shown in Fig. 14 is exceedingly small compared to the sample

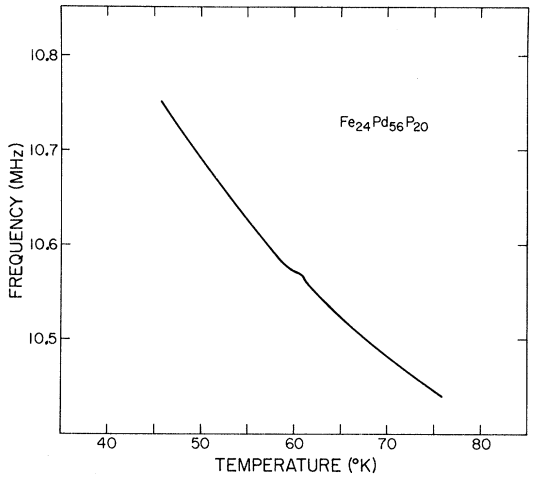

FIG. 14. Frequency measurement for the $Fe_{24}Pd_{56}P_{20}$ alloy.

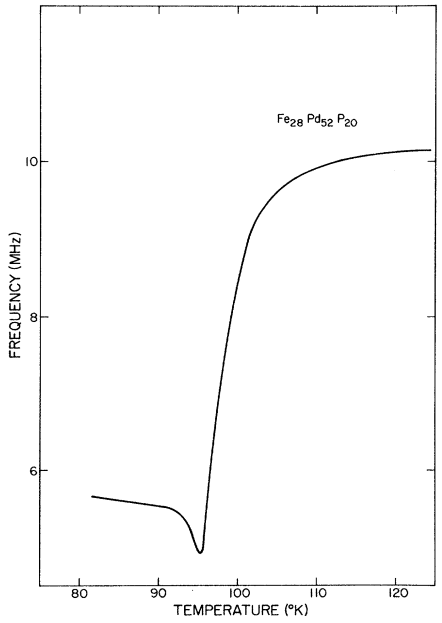

FIG. 13. Frequency measurement for the $Fe_{28}Pd_{52}P_{20}$ alloy.

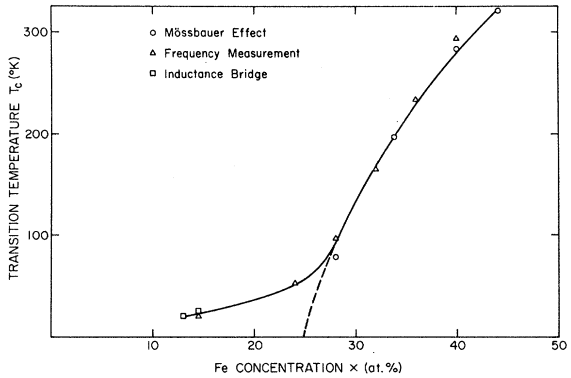

FIG. 15. Magnetic transition temperature vs iron concentration for the amorphous $Fe_xPd_{80-x}P_{20}$ alloys.

with only 4% more Fe. For the alloys with even less Fe, the frequency change is so small it is difficult to accurately determine the transition point. Several alloys of lower Fe concentration were measured with the inductance bridge described earlier. Approximately 100 mg of each sample were used. An extremely small inductance change was observed at the transition temperature.

The transition temperatures determined by these three methods are shown in Fig. 15. The most significant feature of the variation with Fe concentration is the sharp change in slope at about $x \simeq 26$. If the upper portion of the curve were extrapolated, it would appear that there would be no magnetic transition below approximately 25% Fe.

IV. DISCUSSION

A. Mössbauer Effect

1. *Electronic Configuration of* Fe *in the Amorphous* Fe-Pd-P *Alloys*

The relative constancy of isomer shift and average hyperfine field with respect to variation in composition indicates that the electronic state of Fe in these amorphous alloys does not change drastically with concentration, as the measured saturation moment might imply. On the basis of the isomer-shift calibration of Walker *et al.*[23] and the data of Fig. 2, Fe would be assigned an electronic configuration of $3d^{7.1}4s^{0.9}$.

This assumes that the atom is electrically neutral. Since the host is metallic, this is probably a quite reasonable assumption. It is not valid to merely scale the electronic moment with hyperfine field, since the separate contributions are not known. A magnetic moment of $2.1\mu_B$ per Fe atom, approximately independent of concentration, would be compatible with the observed hyperfine field. The decrease in saturation moment at 8.4 kOe observed is attributed to increased difficulty in saturating the alloys as the Fe concentration decreases.

2. *Variation of Hyperfine Field Distribution with* Fe *Concentration*

a. Discussion of possible Pd *d-band polarization.* The nature of the hyperfine field distribution in the amorphous Fe-Pd-P alloys is quite different from that observed in crystalline Fe *Pd* alloys.[20,24] In a series of such alloys ranging in composition from $Fe_{0.4}Pd_{99.6}$ to $Fe_{43}Pd_{57}$, measurements of the Mössbauer spectrum at 4.2 °K (well below all Curie points) showed that the hyperfine field was essentially unique—that is, all six lines in the spectrum had essentially equal linewidth, which was the same as that observed above the Curie point. A rapid increase in the magnitude of the hyperfine field was observed in the range 0–12 at.% Fe, after which the value leveled off at approximately 335 kOe. These observations were shown to be consistent with a long-range polarization of the Pd conduction band. This polarization varies extremely slowly over distances compared to the average spacing between Fe atoms (thus giving a unique field), and does not oscillate in sign. From neutron-diffraction experiments Low[25] has estimated the range of this spin polarization to exceed 10 Å in $Fe_{0.25}Pd_{99.75}$. Although a very large moment per Fe atom is observed ($\sim 10\mu_B$), the moment of the Fe atom itself is only about $3\mu_B$. The remainder resides on the polarized Pd atoms. The maximum value of moment per Pd atom is only about $0.06\mu_B$, but the unusually long-range interaction encompasses many Pd atoms (~ 100).

These results are pertinent to the discussion here because the possibility of this type of polarization has been suggested to explain the high value of μ_{eff} in the Fe-Pd-P alloys[9] and also in related amorphous Pd-Si alloys with dilute Fe [7] or Co [26] impurities. Since $\mu_{eff} \sim 6\mu_B$ in the $Fe_xPd_{80-x}P_{20}$ alloys with $x \gtrsim 25$, it is inconsistent to assume such a large moment could exist on the Fe atom itself.

To contrast the Fe *Pd* results with those obtained here for the amorphous Fe-Pd-P alloys, the most obvious difference is the very broad distribution of hyperfine fields which exists in the amorphous material. On the scale of Fig. 7, the distribution function for a typical Fe *Pd* alloy would be essentially a δ function in comparison with those shown. Second, there is a pronounced increase in the width of this distribution with increasing Fe concentration for the amorphous alloys. The simple model presented in Sec. III showed that a finite width was expected, merely because of the random fluctuations in local atomic arrangement. It was also suggested that one of the dominant effects to be considered in the distribution of hyperfine fields was the electron-transfer effect from phosphorus. Since the P content remains constant, this effect alone cannot explain the increase in width observed in the higher-Fe-concentration alloys.

There are also contributions to the hyperfine field from the conduction electrons, which may become polarized through the Ruderman-Kittel-Kasuya-Yosida (RKKY)[27–29] interaction and contribute to the observed hyperfine field. In Fe *Pd* alloys, this polarization, which normally oscillates in sign with distance from the magnetic moment, becomes so enhanced by the exchange interaction that it no longer oscillates and acquires a very large range.[30] For a long-range interaction of this type, the hyperfine field distribution remains very narrow and merely changes its position with varying concentrations.

The broad hyperfine field distributions shown in Fig. 7 argue strongly against a long-range polariza-

tion of this type. There are also several other reasons for thinking that polarization of the Pd matrix does not play a large role in these amorphous alloys. First of all, the presence of phosphorus as an electron donor should greatly reduce the polarization of the Pd matrix. It is a well-documented fact that Pd tends to assume a diamagnetic state in alloys.[31] Pd often acts in alloying as if 0.6 holes per Pd atom existed in its 4*d* band. In the Pd-H system, for example, at a ratio H/Pd = 0.6 the Pd 4*d* band appears to be completely full, and the material is diamagnetic.[32] This effect is also observed when many other higher-valence elements are substituted into Pd.[31] Specific-heat measurements indicate a low density of states in these alloys. One can also substitute Fe for Pd in Pd-H, up to approximately 10% Fe.[32] A Mössbauer study[33] of two such alloys showed a considerably reduced transition temperature relative to an Fe*Pd* alloy of the same percentage Fe. Hyperfine field and isomer-shift results showed that the Fe atoms retained approximately their same state as in Fe*Pd*, however, It is quite interesting to note that the μ_{eff} obtained from susceptibility measurements was essentially constant in the range 0–9% Fe with the large value of $(5.7-5.9)\mu_B$,[32] although it was clear that the Pd *d* band is completely full.

A similar band-filling effect of this type might be expected for the Fe-Pd-P alloys, and it is unfortunate that the amorphous range does not extend to lower Fe concentrations. Amorphous $Fe_xPd_{80-x}Si_{20}$ alloys can be made in the dilute range (0–7% Fe), however, and show magnetic properties quite similar to the low-Fe-concentration Fe-Pd-P alloys (incomplete saturation, high μ_{eff}, diffuse magnetic transition from magnetization measurements). The host $Pd_{80}Si_{20}$ has a very low susceptibility ($\chi \sim 10^{-7}-10^{-8}$ emu/g),[34] indicating a filled *d* band.

b. Nature of the hyperfine field distribution: relation to Kondo effect. In an attempt to put the discussion of $P(H)$ on a more quantitative basis, we can use the following model: Considering the hyperfine field H as a random variable, we separate the contributions to H into two categories,

$$H = H_1 + H_2 \ , \tag{10}$$

where H_1 represents contributions which are approximately independent of the Fe concentration x, and H_2 the factors which may change appreciably with x. Since the Fe moment appears to be almost constant in magnitude over the composition range, the second group comprises basically contributions from the conduction electrons.

Included in H_1 are the dominant core-polarization term and the smaller effects due to possible orbital and dipolar contributions. The latter should not depend greatly on x. Also in this category are the electron-transfer effects from phosphorus discussed earlier. It was argued there that the probability distribution from these contributions should have the approximate form

$$P_1(H_1) = \frac{1}{(2\pi\Delta_1^2)^{1/2}} \exp\left(-\frac{(H_1-\bar{H}_1)^2}{2\Delta_1^2}\right) . \tag{11}$$

To calculate $P_2(H_2)$ we need a model which represents the most relevant interactions in producing conduction-electron spin polarization. One mechanism is the RKKY interaction between the Fe moments and the conduction electrons. Since the arrangement of the Fe atoms is governed by the radial distribution function, H_2 should be statistically independent of H_1. In such a case the probability distribution for $H = H_1 + H_2$ can be obtained from a convolution of the separate probability distribution functions:

$$P(H) = \int P_1(H')\, P_2(H-H')\, dH' \ . \tag{12}$$

The response of a free-electron gas to a point magnetic moment leads to an oscillatory spin polarization (RKKY interaction):

$$\Phi_{RKKY}(r) = \rho_\uparrow(r) - \rho_\downarrow(r) = \rho_0\left(\frac{\cos 2k_F r}{(2k_F r)^3} - \frac{\sin 2k_F r}{(2k_F r)^4}\right) , \tag{13}$$

where r is the distance from the magnetic moment and k_F is the Fermi wave vector. The RKKY interaction produces a spatially nonuniform spin polarization, and therefore leads to a broadening of the hyperfine field distribution. This effect is quite evident in NMR studies, and was first observed in dilute *Cu*Mn alloys.[35]

In Fig. 8 the width of the central peak in $P(H)$ increases by roughly a factor of 2, which means that broadening effects due to conduction-electron polarization are comparable to those from other factors. The RKKY interaction is capable of effects of this magnitude, as was shown in Mössbauer experiments by Stearns and Wilson.[36] By introducing impurities in the Fe lattice, they were able to verify the oscillatory nature of the conduction-electron spin polarization, although the magnitude was roughly seven times that predicted by Eq. (13). This was presumably due to the neglect of electron-electron interactions in the analysis which leads to the RKKY form factor. It was found that the spin polarization from one Fe atom at a nearest-neighbor Fe nucleus leads to a hyperfine field of approximately 26 kOe. It is clear, therefore, that in the concentration range of the Fe-Pd-P alloys these effects can produce a broadening of sufficient magnitude to agree with experimental results.

A calculation of $P(H_2)$ would then proceed as follows: Knowing ρ_0, k_F, and the Fe arrangement, we can calculate $P(H_2)$ using Eq. (13). Only the average distribution of Fe atoms can be obtained

from the radial distribution function, so the actual calculation would have to consider all possible Fe arrangements weighted with the appropriate probability. This type problem is well suited to numerical methods such as Monte Carlo techniques.

There is one other factor to be considered before embarking on such an approach—the short mean free path of the conduction electrons in a disordered structure. It is known that the amplitude of the magnetization oscillations decreases with decreasing mean free path. This effect can be described qualitatively by the intuitive formula[37]

$$\Phi(r) = \Phi_{\mathrm{RKKY}}(r)\, e^{-r/\Lambda} , \tag{14}$$

where Λ is the mean free path for conduction electrons. This effect was verified by Heeger *et al.*,[38] who observed a decrease in NMR linewidth when nonmagnetic impurities (which decrease the mean free path) were introduced into the *Cu*Mn system. In amorphous materials, the mean free path must be extremely short. It can be estimated from the simple conductivity formula

$$\sigma = ne^2\tau/m . \tag{15}$$

(The measured resistivity of the Fe-Pd-P alloys is in the range 160–180 $\mu\Omega$ cm.) The mean free path Λ is simply $v_F\tau$. Assuming that n and v_F are characteristic of a noble metal such as Cu, we find that $\Lambda \sim 3$ Å (on the order of the interatomic spacing). The range of the RKKY polarization should be drastically reduced in such a situation, and should not extend appreciably beyond nearest and next nearest neighbors.

The complicated numerical approach outlined above, therefore, is not necessary. The arguments of Sec. III can be applied immediately, with the only difference being that α in Eq. (2) comes from the RKKY spin polarization, and n is now the number of Fe nearest neighbors. Again the probability distribution should have a form similar to the Gaussian distribution, with average value $\overline{H}_2$ and standard deviation Δ_2.

In the convolution of $P_1(H_1)$ and $P_2(H_2)$ according to Eq. (12), the resulting shape will again be approximately Gaussian with $\overline{H} = \overline{H}_1 + \overline{H}_2$, $\Delta = \Delta_1 + \Delta_2$. If the RKKY polarization is basically limited to nearest neighbors, $\Delta_2 \propto x^{1/2}(0.8 - x)$ for the $\mathrm{Fe}_x\mathrm{Pd}_{80-x}\mathrm{P}_{20}$ alloys (from the binomial distribution). Therefore,

$$\Delta H = \Delta_1 + \Delta_2[x(0.8 - x)]^{1/2} . \tag{16}$$

The trend in ΔH observed can be well approximated by such a formula with $\Delta_1 = 20$ kOe and $\Delta_2 = 145$ kOe.

One feature of the probability distributions in Fig. 8 which cannot be explained by this simple model is the large "tail" effect seen at low fields. The reason for this discrepancy can be understood as follows: The calculation just outlined would predict the distribution of *saturation* fields which exist in the material. To get the actual $P(H)$ distribution, we must consider the effective fields (dynamical effects) which act on the magnetic moments. For example, in an effective field theory, the actual hyperfine field measured corresponding to a given magnetic moment μ is

$$H = H_{\mathrm{sat}} B_s(\mu h/kT) , \tag{17}$$

where h is the effective (Weiss) field at that site. Our model just proposed has really been concerned with $P(H_{\mathrm{sat}})$. In order to obtain $P(H)$, we must in addition know $P(h)$.

In the amorphous Fe-Pd-P alloys the existence of a Kondo-type resistivity minimum[9] implies that there are spins in low effective fields, even in the concentrated alloys. It has been shown theoretically that the effect of spin-spin correlations is to produce an internal field which suppresses the Kondo effect. If the spins are locked into parallel alignment, the spin-flip–scattering process (which gives rise to the resistivity minimum) cannot occur. The appearance of the "tail" on the observed low-field $P(H)$ distribution is a confirmation of the possibility of a Kondo effect in these amorphous alloys. These smaller hyperfine fields come from Fe atoms which reside in low effective fields and are weakly coupled. These moments are quasifree and can participate in the spin-flip scattering.

3. *Variation of Quadrupole Splitting with* Fe *Concentration*

At first thought it is difficult to assess the meaning of the increase in quadrupole splitting with decreasing Fe concentration shown in Fig. 3. Assuming that the short-range order remains constant, the only change is to gradually replace Pd by Fe. Since the main electrostatic effects are due to phosphorus (because of its large charge contrast), and its concentration is fixed, this variation may seem quite puzzling. The discussions of the previous sections show how a possible resolution of this question may be achieved. From the isomer-shift and hyperfine field results, the electronic state of the Fe atoms remains roughly unchanged throughout the composition range. However, it seems reasonable to assume that the 4*d* shell of Pd is full. If we think of phosphorus as an electron donor to palladium, then the electron transfer depends only on the concentration of Pd. Hence the local-charge perturbation should be proportional to $(0.8 - x)$. Since electric field effects are proportional to this quantity, $q(x) \propto (0.8 - x)$. Actually this predicts that the quadrupole splitting would vanish at $x = 0.8$, whereas in reality we would undoubtedly have a small quadrupole splitting even in an amorphous $\mathrm{Fe}_{80}\mathrm{P}_{20}$ alloy. Thus

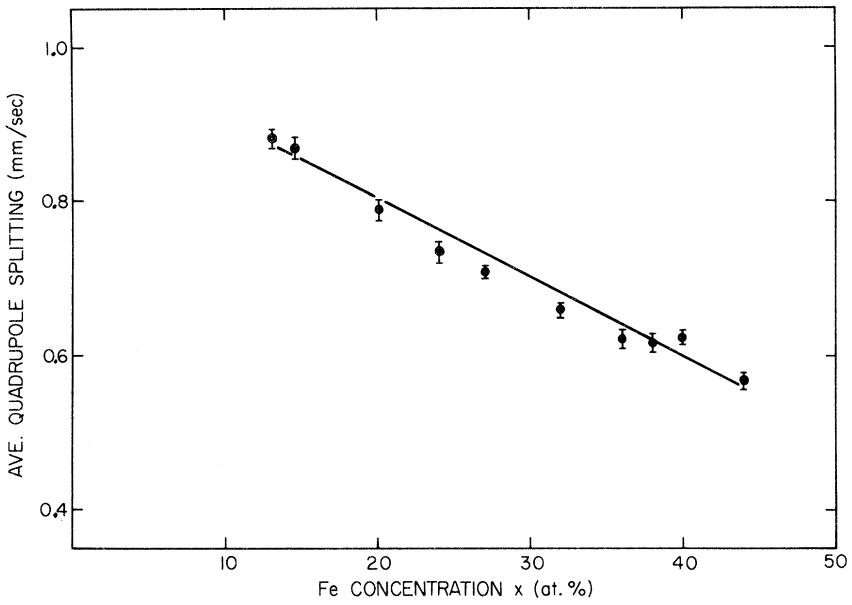

FIG. 16. Quadrupole splitting vs iron concentration according to Eq. (18).

we should write

$$\left|\tfrac{1}{2}e^2qQ\right| = Q_0(0.8 - x) + Q_1 \,. \tag{18}$$

Figure 16 shows the curve for $Q_0 = 1.0$ mm/sec, and $Q_1 = 0.2$ mm/sec. Any numerical agreement with such a simple model is clearly in part fortuitous. However, the model is consistent with the earlier discussion and accounts for an effect which seems quite mysterious otherwise.

B. Magnetic Properties

1. *High*-Fe-*Concentration Alloys*: $x \gtrsim 25$

From the experimental data presented in Sec. II, in particular the transition temperature curve of Fig. 15, it seems appropriate to divide the discussion of the magnetic properties of the amorphous Fe-Pd-P alloys into two sections. In this section we will discuss the alloys with $25 < x \leq 44$. In this range the alloys appear to be good examples of amorphous ferromagnets. Hence they are good candidates for evaluating several recent theories of the magnetization in this type of material.

For these alloys we can use the hyperfine field distributions obtained to study the dependence of magnetization on temperature. Since $H\alpha\langle S_z\rangle$, a plot of $\bar{H} = \int_0^\infty P(H)\,H\,dH$ vs temperature should be a measure of the zero-field magnetization of the sample. We can therefore compare the experimentally observed magnetization with that predicted theoretically.

Handrich[39] has recently given a treatment of the amorphous ferromagnet on the basis of the molecular field approximation. Starting from the Heisenberg-Dirac Hamiltonian,

$$H = -\sum J_{ij}\vec{S}_i \cdot \vec{S}_j \tag{19}$$

the amorphous nature of the material is taken into account by allowing random fluctuations in the exchange integrals J_{ij}. It is found that the effect of these fluctuations is to produce the following equation of state for the (reduced) magnetization:

$$\sigma = \tfrac{1}{2}\{B_s[(1+\delta)x] + B_s[(1-\delta)x]\} \,, \tag{20}$$

where $x = 3S/(S+1)(\sigma/\tau)$, $\tau = T/T_c$, and δ is a measure of the fluctuations. For $\delta > 1$ no ferromagnetism exists at any temperature.

A numerical calculation was performed for various values of δ and is compared with the experimental data in Fig. 17. The effect of increasing structure fluctuations is a decrease in the hyperfine field, while the Curie point remains unchanged. The magnetization has infinite slope at $T = T_c$. The failure of the theory to account for the low-temperature behavior is a characteristic of all molecular field theories, and results from the inability to predict the low-temperature excitations (spin waves). Qualitatively, however, the prediction that the fluctuations have reduced the magnetization relative to the order state ($\delta = 0$) seems to be verified.

A recent calculation by Montgomery *et al*,[40] treats the disordered Heisenberg ferromagnet by a Green's-function technique. Although this theory is not strictly applicable to an amorphous material but rather a disordered alloy, the general conclusions are expected to remain valid. The density of spin wave states, the ferromagnetic Curie temperature, and the magnetization were found as a function of disorder. The randomness of the alloy

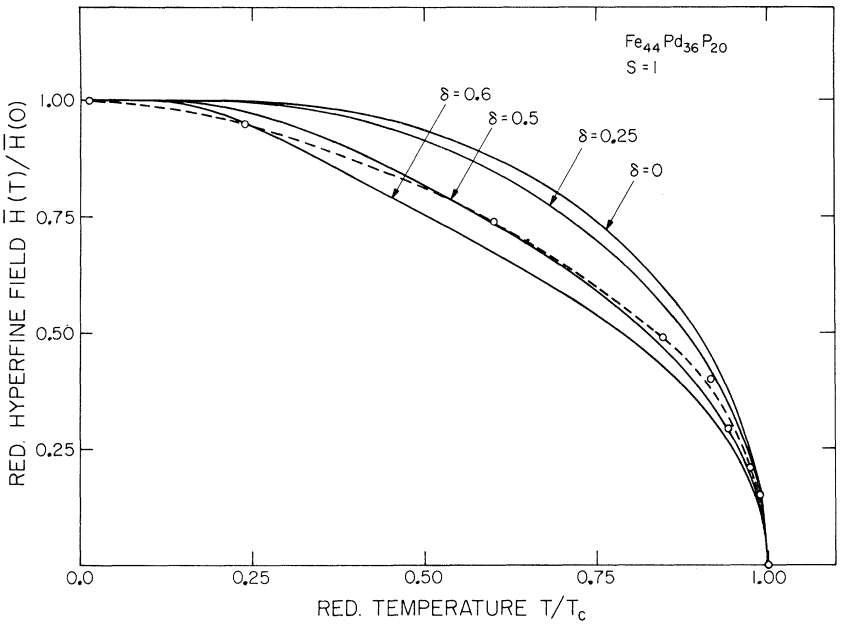

FIG. 17. Comparison of experimental results (dashed line) with Eq. (20) for the $Fe_{44}Pd_{36}P_{20}$ alloy.

was taken into account by defining a parameter P such that

$$P = j^2/3J_0^2 ,$$

where j^2 is the mean-square deviation in exchange integrals from the average value J_0. The parameter P thus defined is a measure of the disorder analogous to δ in Handrich's molecular field theory. It was found that the density of spin wave states changes markedly with disorder. The main effect of increasing P is to introduce a low-energy peak in the density of states, which results in the reduction in Curie temperature according to

$$T_c = T_0(1 - (6/Z)P) , \qquad (21)$$

where T_0 is the transition temperature for the ordered case and Z is the number of nearest neighbors. The magnetization curves retain their characteristic shape and are merely flattened slightly from the perfect crystal case.

It is difficult to quantitatively assess the agreement of this approach with the amorphous case, since the numerical calculations involved must be made for a specific type of lattice. Nevertheless, the general conclusion that the magnetization is flattened relative to the perfect-crystal case is seemingly valid. For example, in crystalline Fe at $T/T_c = 0.25$, the magnetization has dropped only 2%, while for the amorphous alloys shown in Fig. 17 it is reduced ~ 5–6%.

2. *Low-Fe-Concentration Alloys*: $x \lesssim 25$

a. Critical concentration effects. The experimental results point to the existence of a critical concentration for ferromagnetism in the amorphous Fe-Pd-P alloys at approximately 25% Fe. There have been several calculations of critical concentration for crystalline lattices based on the Heisenberg-Dirac Hamiltonian. Elliot *et al.* [41] have shown that this critical concentration is independent of the spin S or the strength of exchange coupling J, and depends only on the topology of the lattice. Moreover, x_c (the critical concentration) is the same for both the Heisenberg and Ising models. To show this, the high-temperature susceptibility χ was expanded in a power series of x, the concentration. The critical concentration x_c is obtained from an analysis of the radius of convergence of this power series. The following values were found for the simple-cubic (sc), body-centered-cubic (bcc), and face-centered-cubic (fcc) lattices: $x_c = 0.28$, 0.22, and 0.18, respectively.

Sato *et al.* [42] have also discussed critical concentration effects based on other approximations to the Heisenberg Hamiltonian. They find that the molecular field approximation, which predicts $T_c \propto x$ (and therefore has no critical concentration), is completely inadequate in treating the case of dilute magnetic alloys with short-range interactions. This failure of the MFA is due to the averaging technique adopted. One can show, in fact, that the molecular field theory is exact only in the limit of Z (the number of nearest neighbors) becoming infinite. The neglect of short-range order effects in the MFA is manifested in its inability to predict the curvature in $1/\chi$ vs T plots just above T_c, and also in the prediction that the magnetic contribution to the specific heat drops abruptly to zero above T_c.

TABLE IV. Critical concentration for nearest-neighbor interactions. (Z is the coordination number of the lattice.)

Lattice	Expansion method	Average coordination number	Cluster variation
sc($Z=6$)	0.28	0.333	0.20
bcc($Z=8$)	0.22	0.25	0.143
fcc($Z=12$)	0.18	0.166	0.091

Several other effective field theories, which do attempt to treat short-range order effects, are considerable improvements in accounting for these effects. It appears that the longer the range of the interaction, the more applicable the MFA may be. This may be the reason for its semiquantitative success in Fe*Pd*, where there are unusually long-range interactions. In amorphous materials, where short-range interactions are dominant, the MFA is not expected to be a good approximation.

Two such predictions for critical concentrations are given by the average coordination number (ACN) method and the cluster variation (CV) theory.[42] The ACN treatment is essentially a generalization of Bethe's method for dealing with order-disorder phenomena in alloys. It is found that a critical concentration is reached when $xZ=2$. The other method (CV) gives $x_c=1/(Z-1)$. Table IV gives a summary and comparison of these estimates for the three different methods.

In the amorphous Fe-Pd-P alloys there is no lattice on which to count nearest neighbors. However, it is known from the RDF that the metal-metal concentration number is about 10–11. With this value for Z, the predicted critical concentration would be in the range of 10–12%. Since only 0.8 of the atoms are metallic, x_c should be between 8–16 at.% Fe. Experimentally $x_c \cong 25\%$. It is reasonable that x_c for an amorphous structure should be greater than the ordered case, and recent theories predict that the Curie point of the amorphous structure is reduced relative to the ordered case.

b. Evidence against superparamagnetism. Below the critical concentration, there is no long-range ferromagnetism. The observation of a hyperfine field shows that some kind of local magnetic order persists, however. If the alloys in this range are indeed superparamagnetic, we can estimate the average "cluster" size and number of Fe atoms per cluster from the observed μ_{eff} value. In the paramagnetic region,

$$\chi = N\mu^2/3k(T-\theta)\,, \tag{22}$$

where N is the number of clusters per unit volume and μ is the moment per cluster. Assuming there are n Fe atoms per unit volume and z Fe atoms per cluster, then $N=n/z$ and $\mu \cong z\mu_{\text{Fe}}$. In this situation

$$\chi = \frac{n}{z}\,\frac{(z\mu_{\text{Fe}})^2}{3k(T-\theta)} = z\,\frac{n\mu_{\text{Fe}}{}^2}{3k(T-\theta)} = z\chi_{\text{indep}}\,. \tag{23}$$

Thus by grouping into clusters of z atoms each, the susceptibility is increased by a factor of z, or the effective moment by a factor $z^{1/2}$. Since $\mu_{\text{eff}} \cong 6$ for the amorphous Fe-Pd-P alloys and $\mu_{\text{Fe}} \cong 3$, there are only about four Fe atoms per cluster on the average. If Pd contributed to the net moment, this value would be even smaller. In the composition range $13 \leq x \leq 25$, the clusters would contain 16–32 atoms on the average. Since the RDF indicates an atomic radius of 1.4–1.5 Å,[9] 20 atoms would occupy a volume V of only $\sim 3\times 10^{-22}$ cm^3.

If the clusters are noninteracting, thermal fluctuations will occur at a rate

$$f_{\text{relax}} = f_0 e^{-KV/kT} \cong 10^9\, e^{-KV/kT}\ \text{sec}^{-1}\,. \tag{24}$$

In order to observe a hyperfine field, $f_{\text{relax}} < f_{\text{Larmor}}$. For Fe^{57}, $f_{\text{Lamor}} \cong 10^7$ sec^{-1}. To be consistent with the result that a hyperfine field is observed at 4.2 °K, we find from Eq. (24) that the condition on the anisotropy energy constant K is $K \gtrsim 10^{-7}$ erg/cm^3. This is greater than an order of magnitude larger than Fe.[43] It would be difficult to explain such a large value for the amorphous alloys, where there would seem to be no crystallographic axis to even define a preferred direction. One would expect the anisotropy energy to be much lower than in the crystalline case. In fact, amorphous Fe-P-C alloys exibit magnetoelastic properties which indicate this is the case.[44]

Another characteristic effect seen in superparamagnetic materials is noticeably absent in the amorphous Fe-Pd-P alloys with $x < 25$. Because of the distribution of cluster sizes, there are always a wide range of transition temperatures evident in the Mössbauer spectrum. If the $Fe_{24}Pd_{56}P_{20}$ alloy were superparamagnetic, we would expect to see some evidence of hyperfine splitting at 77 °K, since its transition temperature is just below this temperature ($T_c \sim 60$ °K). Similarly, for $Fe_{14}Pd_{66}P_{20}$ at 4.2 °K, some quadrupole component should be seen from paramagnetic Fe atoms which happen to be in an uncoupled state. Furthermore, the frequency and inductance-bridge results indicate a rather well-defined transition temperature, which seems to correspond to the value extrapolated from Mössbauer effect. If the alloys were superparamagnetic, the transition temperature obtained from the two different techniques would vary greatly because of the difference in measurement time. In the Mössbauer effect, the average hyperfine field is obtained over a Larmor period ($\sim 10^{-7}$ sec), while the inductance bridge is essentially a static measurement (oscillator frequency = 1 kHz). For example, small particles of nickel ferrite ($NiFe_2O_4$) of average size

168 Å show paramagnetic behavior in magnetization measurements at all temperatures, but exhibit a stable hyperfine field pattern in Mössbauer experiments up to 628 °K, where a gradual narrowing of the pattern sets in.[45] The corresponding Curie point of the bulk material is 858 °K.

*c. Nature of the magnetic state: comparison with the Au*Fe *system.* The magnetic properties of the amorphous Fe-Pd-P alloys are in many ways analogous to those observed in *Au*Fe alloys.[46–54] Below approximately 16% Fe, the alloys respond only weakly to an external magnetic field. The susceptibility results give a large μ_{eff}, which approaches the value corresponding to $S = \frac{5}{2}$ ($\mu_{eff} = 5.92$) near this critical concentration. The transition-temperature–vs–iron-concentration curve also shows a sharp change in slope in this region, as shown in Fig. 18.

The reason for the apparent similarity between the two systems is not obvious at first sight. However, the model for the magnetism in these alloys proposed earlier shows why the analogy may be expected. In that discussion it was argued that the effects of Pd 4*d* electron polarization are negligible because of electron transfer from phosphorus. If the 4*d* shell of Pd is filled, it has the same electronic configuration as Ag, except for a slight difference in *s* electron density. In this model phosphorus plays no direct role in the magnetism except to fill the 4*d* shell of Pd and provide possible conduction electrons to the system. It is well established that alloys of 3*d* transition metals (Cr, Mn, Fe, or Co) with elements of the I*B* group (Cu, Ag, Au) show anomalous magnetic properties.[55] The systems *Cu*Fe and *Au*Fe are good examples of this effect. It would be interesting to compare the magnetic properties of the amorphous Fe-Pd-P alloys with *Ag*Fe alloys. Unfortunately, Fe is only very slightly soluble in Ag (~ 0.0004% Fe).[56] Therefore a direct comparison is impossible.

V. SUMMARY AND CONCLUSIONS

Alloys of the form $Fe_x Pd_{80-x} P_{20}$ ($13 \leq x \leq 44$) have been quenched from the liquid state into an amorphous structure using the "piston and anvil" technique. Mössbauer-effect measurements have been used to determine the distribution of hyperfine fields in these materials as a function of composition and temperature. Despite the presence of a combined electric quadrupole and magnetic interaction in the magnetically ordered alloys, the Mössbauer spectra can be analyzed in terms of a hyperfine field distribution alone. This simplification arises from the fact that structure fluctuations in the amorphous alloys lead to a completely random angle between the magnetic field direction and the principle axis of the efg at the nucleus. The only effect of the electric quadrupole interaction is therefore to broaden the observed six-peak spectrum resulting from the magnetic hyperfine interaction. The hyperfine field distributions in the amorphous Fe-Pd-P alloys are found to be extremely broad (width ~ 100 kOe), with a maximum at approximately 290 kOe which is relatively independent of concentration. The increased width observed in the higher-Fe-concentration alloys results from the spin polarization of the conduction electrons. From these results it has been concluded that the electronic configuration of Fe remains approximately constant throughout the entire composition range. The magnetic moment per Fe atom is about $2\mu_B$. The Pd atoms appear to play little role in the magnetism, since the Pd 4*d* shell has been filled due to electron transfer from phosphorus. The quadrupole splitting observed above the transition temperature is consistent with this model. Phosphorus thus plays a dual role in affecting the Pd *d* band and also in allowing the formation of the amorphous structure.

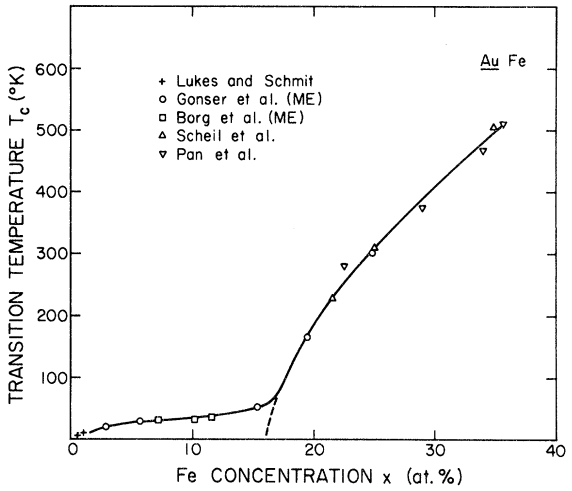

FIG. 18. Magnetic transition temperature vs iron concentration in $Au_{1-x}Fe_x$ alloys.

On a microscopic scale, there is a drastic change in the magnetic properties of the Fe-Pd-P alloys at approximately 26% Fe. The transition-temperature–vs–Fe-concentration curve shows a sharp change in slope in this region. Above this critical concentration, the alloys are amorphous ferromagnets. The temperature dependence of the magnetization for these alloys agrees fairly well with recent theoretical predictions. Below the critical concentrations, the short-range exchange interactions which produce the ferromagnetism are unable to establish a long-range magnetic order. The local magnetic ordering which occurs must be due to some indirect exchange interactions through the conduction electrons. In many respects, the be-

havior of the Fe-Pd-P amorphous alloys parallels that observed in the *Au*Fe system. This might be expected, since the electronic configuration of Pd is the same as the noble metal Ag if its *d* shell is filled.

One of the most significant features of the amorphous state is the fact that correlations between neighboring spins in such a material are greatly reduced. This makes possible the existence of Kondo spin-flip scattering even in quite concentrated alloys. Only those spins which are in weak effective fields can contribute to the Kondo effect. The hyperfine field distributions obtained experimentally confirm the existence of such weakly coupled spins.

This model of Fe atoms interacting on a random lattice can explain the observed magnetic properties without introducing any concepts such as superparamagnetism or concentration-dependent magnetic moments for the Fe atoms. It also shows the connection between the magnetism in such apparently dissimilar amorphous alloys as ferromagnetic $Fe_{80}P_{13}C_7$ and $Fe_x Pd_{80-x} Si_{20}$ $(0 < x \leq 7)$. The large critical concentration observed in the Fe-Pd-P alloys provides further support for the statement that spin-spin correlations are greatly reduced in the amorphous state. This seems to be more than just a question of a short mean free path for the conduction electrons, since the alloys can be magnetically ordered in the dilute region.

To investigate the magnetic ordering in the less-concentrated alloys ($x < 25$), Mössbauer experiments in large external fields should be quite useful. Specific-heat measurements at low temperatures should also show a large contribution from the quasifree spins in weak effective fields. The detailed analysis may be quite complicated, however, since there is no base alloy ($Pd_{80}P_{20}$) to use in the subtraction of the nonmagnetic contributions.

Finally, it should be noted that the Mössbauer effect is at present the only technique by which one can determine the complete distribution of hyperfine fields in these materials. The unusual widths of the distributions would make an NMR absorption, for example, so broad that no useful information could be obtained. Thus it represents a unique tool in the study of magnetism in amorphous materials, and should become even more important in future developments in this field.

ACKNOWLEDGMENT

The authors wish to express their appreciation to Professor Pol Duwez for his advice and encouragement throughout this work.

---

*Work supported by the U. S. Atomic Energy Commission.

[1]A. I. Gubanov, Fiz. Tverd. Tela 2, 502 (1960) [Sov. Phys. Solid State 2, 468 (1961)].

[2]S. Mader and S. Nowick, Appl. Phys. Letters 7, 57 (1965).

[3]C. C. Tsuei and Pol Duwez, J. Appl. Phys. 37, 435 (1966).

[4]Pol Duwez and S. C. H. Lin, J. Appl. Phys. 38, 4096 (1967).

[5]K. Tanura and H. Endo, Phys. Letters 29A, 52 (1969).

[6]C. C. Tsuei, G. Longworth, and S. C. H. Lin, Phys. Rev. 170, 603 (1968).

[7]R. Hasegawa, J. Appl. Phys. 41, 4096 (1970).

[8]A. K. Sinha, J. Appl. Phys. 42, 338 (1971).

[9]P. L. Maitrepierre, Ph.D thesis (California Institute of Technology, 1969) (unpublished).

[10]P. L. Maitrepierre, J. Appl. Phys. 40, 4826 (1969).

[11]P. Pietrokowsky, Rev. Sci. Instr. 34, 445 (1962).

[12]S. Rundqvist, Arkiv Kemi 20, 67 (1963).

[13]J. Kondo, Progr. Theoret. Phys. (Kyoto) 32, 37 (1964).

[14]W. L. Trousdale, C. J. Song, and G. Longworth, in *Mössbauer Effect Methodology* (Plenum, New York, 1966), Vol. 2, pp. 77–83.

[15]R. M. Bozorth, *Ferromagnetism* (Van Nostrand, New York, 1951).

[16]E. Kankeleit, in *Mössbauer Effect Methodology* (Plenum, New York, 1965), Vol. 1, pp. 47–66.

[17]R. S. Preston, S. S. Hanna, and J. Heberle, Phys. Rev. 128, 2207 (1962).

[18]L. R. Newkirk, Ph.D. thesis (California Institute of Technology 1970) (unpublished).

[19]G. K. Wertheim, *Mössbauer Effect: Principles and Application* (Academic, New York, 1964).

[20]P. P. Craig, B. Mozer, and R. Segnan, Phys. Rev. Letters 14, 895 (1965).

[21]B. D. Dunlap and J. G. Dash, Phys. Rev. 155, 460 (1966).

[22]J. S. Smart, *Effective Field Theories of Magnetism* (Saunders, Philadelphia, 1966).

[23]L. R. Walker, C. K. Wertheim, and V. Jaccarino, Phys. Rev. Letters 6, 98 (1961).

[24]T. A. Kitchens and W. L. Trousdale, Phys. Rev. 174, 606 (1968).

[25]G. Low, in *Proceedings of the International Conference on Magnetism, Nottingham, England*, 1964 (The Institute of Physics and the Physical Society, Berkshire, England 1965).

[26]M. E. Weiner, Ph.D. thesis (California Institute of Technology, 1968) (unpublished).

[27]M. A. Ruderman and C. Kittel, Phys. Rev. 96, 99 (1954).

[28]T. Kasuya, Progr. Theoret. Phys. (Kyoto) 16, 45 (1956).

[29]K. Yosida, Phys. Rev. 106, 893 (1957).

[30]B. Giovanni, M. Peter, and J. R. Schrieffer, Phys. Rev. Letters 12, 736 (1964).

[31]E. Vogt, in *Magnetism and Metallurgy* (Academic, New York, 1969), Vol. I, Chap. VI.

[32]J. P. Burger, Ann. Phys. (Paris) 9, 345 (1964).

[33]W. C. Phillips and C. W. Kimball, Phys. Rev. 165, 401 (1968).

[34]R. Hasegawa and C. C. Tsuei, Phys. Rev. B 2, 1631 (1970).

[35]J. Owen, M. Browne, W. D. Knight, and C. Kittel,

Phys. Rev. 102, 1501 (1956).
[36]M. B. Stearns and S. S. Wilson, Phys. Rev. Letters 13, 313 (1964).
[37]P. G. de Gennes, J. Phys. Radium 23, 630 (1962).
[38]A. J. Heeger, A. P. Klein, and P. Tu, Phys. Rev. Letters 17, 803 (1966).
[39]K. Handrich, Phys. Status Solidi 32, K55 (1969).
[40]C. G. Montgomery, J. I. Kruger, and R. M. Stubbs, Phys. Rev. Letters 25, 669 (1970).
[41]R. J. Elliot, B. R. Heap, D. J. Morgan, and G. S. Rushbrooke, Phys. Rev. Letters 5, 366 (1960).
[42]H. Sato, A. Arrott, and R. Kikuchi, J. Phys. Chem. Solids 10, 19 (1959).
[43]D. H. Martin, *Magnetism in Solids* (MIT Press, Cambridge, 1967).
[44]Pol Duwez (private communication).
[45]W. J. Schuele, S. Shtrikman, and D. Treves, J. Appl. Phys. 36, 1010 (1965).
[46]A. R. Kaufmann, S. T. Pan, and J. R. Clark, Rev. Mod. Phys. 17, 87 (1945).
[47]W. E. Henry, Phys. Rev. Letters 11, 468 (1963).
[48]P. P. Craig and W. A. Steyert, Phys. Rev. Letters 13, 802 (1969).
[49]U. Gonser, R. W. Grant, C. J. Meecham, A. H. Muir, Jr., and H. Wiedersich, J. Appl. Phys. 36, 2124 (1965).
[50]R. J. Borg, R. Booth, and C. E. Violet, Phys. Rev. Letters 11, 464 (1963).
[51]C. E. Violet and R. J. Borg, Phys. Rev. 149, 540 (1966).
[52]O. S. Lutes and J. L. Schmidt, Phys. Rev. 134, A676 (1964).
[53]E. Scheil, H. Specht, and E. Wachtel, Z. Metallk. 49, 590 (1958).
[54]S. T. Pan, A. R. Kaufman, and F. Bitter, J. Chem. Phys. 10, 318 (1942).
[55]A. N. Gerritsen, Physica 25, 489 (1959).
[56]M. Hansen, *Constitution of Binary Alloys* (McGraw-Hill, New York, 1966), p. 20.

PHYSICAL REVIEW B VOLUME 5, NUMBER 3 1 FEBRUARY 1972

Effect of Pressure on the Ferromagnetic Transition of $MnAs_xSb_{1-x}$ Solid Solutions*

L. R. Edwards and L. C. Bartel
Sandia Laboratories, Albuquerque, New Mexico 87115
(Received 28 July 1971)

The ferromagnetic transition temperatures of $MnAs_xSb_{1-x}$ solid solutions for $0 \leq x \leq 1$ have been measured as a function of pressure up to 4.5 kbar. Previous work has shown that for the solid solutions in the concentration range $0.9 \lesssim x \leq 1$ the magnetic transition is first order and is accompanied by a hexagonal-to-orthorhombic structure transformation, while for $0 \leq x \lesssim 0.9$ the magnetic transition is second order with no structural change. We have found that the initial pressure derivative of the transition temperature ($\partial T_c/\partial P$) changes discontinuously in the narrow concentration range $0.87 \lesssim x \leq 0.90$, further demarcating the first- and second-order regions. We also find that substituting Sb for As in the first-order region increases the critical pressure P_c which stabilizes the orthorhombic phase to the lowest temperature. This further supports Goodenough's observation of a critical molar-volume range in which the first-order transformation occurs. The solid solutions which exhibit second-order behavior are analyzed using an itinerant-electron ferromagnet model.

I. INTRODUCTION

The isomorphic metallic compounds MnAs and MnSb have different magnetic properties which are believed to be due to differences in the Mn-Mn separation distance. For increasing temperature, MnAs exhibits a first-order ferromagnetic (FM) to paramagnetic (PM) transition at 313 °K which is accompanied by a change in crystal symmetry from the hexagonal NiAs structure ($B8_1$) to the orthorhombic MnP structure ($B31$). (Hereinafter we use FM to denote ferromagnetic, ferromagnet, or ferromagnetism, and similarly for PM.) On further heating, a second-order transition involving a change from a low-spin PM to a high-spin PM phase and a change in crystal symmetry from the orthorhombic ($B31$) to hexagonal structure[1] ($B8_1$) is observed at 398 °K. On the other hand, MnSb has a second-order FM to PM transition at 572 °K with the crystal structure remaining hexagonal ($B8_1$) through the transition.[2] A complete series of solid solutions is formed by MnAs and MnSb in which the hexagonal lattice parameters decrease monotonically from MnSb to MnAs.[3]

The various magnetic transition temperatures and crystal structures of the solid solutions, $MnAs_xSb_{1-x}$ as reported by Sirota and Vasilev[4] and Goodenough *et al.*[5] are summarized in Fig. 1. Here, for increasing temperature, T_c denotes the FM-to-PM transition temperature, T' denotes the PM-to-PM transition temperature at which the effective moment decreases, and T_t is a PM-to-PM transition temperature at which the effective moment increases and the crystal structure changes